

NBI-HE-96-19

hep-th/9604152

April, 1996

MULTILOOP WORLD-LINE GREEN FUNCTIONS FROM STRING THEORY

Kaj Roland ¹ AND Haru-Tada Sato ²

*The Niels Bohr Institute, University of Copenhagen
Blegdamsvej 17, DK-2100 Copenhagen, Denmark*

Abstract

We show how the multiloop bosonic Green function of closed string theory reduces to the world-line Green function as defined by Schmidt and Schubert in the limit where the string world-sheet degenerates into a Φ^3 particle diagram. To obtain this correspondence we have to make an appropriate choice of the local coordinates defined on the degenerate string world sheet. We also present a set of simple rules that specify, in the explicit setting of the Schottky parametrization, which is the corner of moduli space corresponding to a given multiloop Φ^3 diagram.

¹Supported by the Carlsberg Foundation, roland@nbivms.nbi.dk

²Fellow of the Danish Research Academy, sato@alf.nbi.dk

1 Introduction

The relation between string theory and field theory has been investigated in considerable detail over the last few years. Any string theory reduces to an effective field theory in the limit where the inverse string tension $\alpha' \rightarrow 0$. But string theory also manages to organize the scattering amplitudes in a very compact form, and this makes the detailed investigation of the field theory limit both non-trivial and potentially very useful.

For example, Bern and Kosower obtained a set of simple rules for the calculation of one-loop amplitudes in pure Yang-Mills theory by systematically analyzing the field theory limit of a suitable heterotic string theory [1]. These rules involved only Φ^3 -like particle diagrams and provided a very significant improvement in computational efficiency over traditional Feynman diagram techniques. In terms of field theory the rules were subsequently seen to correspond to an ingenious combination of background field gauge and Gervais-Neveu gauge [2]. Bern-Kosower rules were also obtained for gravity [3], where the improvement over traditional techniques was even more spectacular.

Later on, Strassler obtained the Bern-Kosower rules directly from a first-quantized world-line formulation of one-loop Yang-Mills theory [4]. This particle approach has been applied to several other theories at the one-loop level [5] and has also been generalized to multiloop Φ^3 -theory [6] and QED [7] by Schmidt and Schubert and to multiloop scalar QED by Daikouji, Shino and Sumino [8].

It would be interesting to find multiloop generalizations of the Bern-Kosower rules also for Yang-Mills theory. To solve this problem it seems very likely that one will need some input from string theory –after all, the subtle combination of gauge choices inherent in the one-loop Bern-Kosower rules would have been quite hard to discover without the help of string theory. On the other hand, a direct generalization of the Bern-Kosower analysis to more than one loop is not straightforward [9],[10], due to the complicated nature of the (super) moduli space of higher genus Riemann surfaces. From this point of view the multiloop world-line formalism seems the more promising one. Thus, both the string approach of Bern and Kosower and the particle approach of Strassler may be

useful, each in its own way.

In this paper we bring the two points of view closer together by showing how the multiloop bosonic world-line Green functions of particle theory, as defined by Schmidt and Schubert [6], can be obtained from the known form of the bosonic world-sheet Green function in string theory [11]. Unlike in string theory, no universal expression for the Green function at any higher loop order is known in particle theory. After all, many topologically inequivalent Φ^3 vacuum diagrams exist at high loop order, and likewise there are many topologically inequivalent ways of inserting two external legs on a given vacuum diagram. But for any insertion of two external legs in a specific vacuum diagram, corresponding to any given 2-point $(m + 1)$ -loop Φ^3 diagram, we should be able to reproduce the particle Green function from the string Green function by approaching the singular point at the boundary of string moduli space where the string world-sheet degenerates into the desired Φ^3 particle diagram.

We do this by a two-step procedure: To approach the singular point, where the surface degenerates into a world-line diagram, we first have to identify the neighbourhood of the singular point; i.e. the corner of moduli space where the string world sheet, which is a two-punctured genus $m + 1$ Riemann surface, looks “almost” like the desired Φ^3 particle diagram, i.e. consists of cylinders, very long in units of the diameter, that are joined together at the vertices. Such a corner of moduli space is defined by letting the $3m + 2$ complex string moduli approach an appropriate limit, known as a *pinching limit*. In the corner of moduli space defined by the pinching limit, the mapping of string moduli into Schwinger Proper Times (SPTs) of the particle diagram can be identified. Since SPTs have dimension of $(\text{length})^2$, they are all proportional to α' . The formal scaling limit, leading to the particle diagram, is then obtained by taking $\alpha' \rightarrow 0$, keeping all SPTs fixed at finite values. We refer to this as the *field theory limit* pertaining to the given Φ^3 diagram.

The procedure for obtaining the particle Green function is this: Evaluate the string Green function $G_{\text{str}}^{(m)}(z_1, z_2)$ in the pinching limit pertaining to the Φ^3 -diagram in question. By taking the formal field theory limit $\alpha' \rightarrow 0$, keeping all SPTs fixed, we obtain the

particle Green function, $\tilde{G}_B^{(m)}(\tau_1, \tau_2)$, as follows

$$G_{\text{str}}^{(m)}(z_1, z_2) \xrightarrow{\alpha' \rightarrow 0} \frac{1}{\alpha'} \tilde{G}_B^{(m)}(\tau_1, \tau_2) + \text{finite} . \quad (1.1)$$

However, there is an important qualification to this statement: As is well known, the bosonic Green function in string theory is not a scalar function of the two arguments; instead it depends on which choice of local coordinates we make on the Riemann surface in the vicinity of the two punctures where the operators are inserted. For this reason, we will not obtain the particle Green function from the string Green function in the field theory limit, as in (1.1), unless we make a *proper choice of local coordinate* in the vicinity of the punctures for the degenerate world-sheet representing the Φ^3 particle diagram in question.

In this paper we present a general prescription on how to choose the local coordinates for any degenerate world-sheet resembling a Φ^3 diagram, so as to obtain the desired relation (1.1). We then proceed to verify eq. (1.1) and our prescription, in particular, in some explicit examples. In their paper [6], Schmidt and Schubert found a very elegant form for the particle Green function pertaining to a large class of diagrams, namely any diagram obtained by inserting $2m + 2$ external legs on a given circle and then joining together m pairs of these legs by the insertion of an internal propagator to form a total of $m + 1$ loops. As we choose different orderings of the $2m + 2$ external legs inserted on the circle, many topologically different 2-point $(m + 1)$ -loop diagrams are obtained. We show how the string Green function can be reduced to the Schmidt-Schubert particle Green function for this whole class of diagrams.

Other particle Green functions can be obtained if one (or both) of the external legs is inserted on one (or two) of the internal propagators instead of on the circle. Generalizing the derivation of Schmidt and Schubert, we also find the particle Green functions corresponding to these classes of diagrams, and we show that they, too, are obtained from the universal expression of the string Green function by taking the relevant field theory limit and using our prescription for the choice of local coordinates.

Thus, we analyze all possible insertions in any Φ^3 vacuum diagram that can be ob-

tained by joining together m pairs of legs inserted on a circle. (We shall refer to this as a Schmidt-Schubert type vacuum diagram). For $m \leq 4$ this exhausts all one-particle irreducible possibilities. For $m \geq 5$ more complicated vacuum diagrams can be imagined, but we do not attempt an analysis of these diagrams.

The paper is organized as follows: In section 2 we present the bosonic Green function in string theory and show how to identify the pinching limit corresponding to any given Φ^3 -diagram, using the Schottky parametrization [12] of Riemann surfaces. We also define the mapping of moduli into SPTs and present our prescription for choosing the local coordinates around the punctures. In section 3 we consider the various particle Green functions that describe all possible insertions in a Φ^3 vacuum diagram of the Schmidt-Schubert type, and in section 4 we recover these Green functions from the string Green function through the relevant field theory limits. Finally, section 5 contains our conclusions, and we also comment on some of the problems that remain to be solved before a string-based set of Bern-Kosower like rules can be obtained for multiloop Yang-Mills theory.

2 The Green Function in String Theory

The bosonic Green function in closed string theory at genus $m + 1$ can be defined as the two point function

$$G_{\text{str}}^{(m)}(P_1, P_2) = \langle X(w_1 = 0)X(w_2 = 0) \rangle , \quad (2.1)$$

evaluated on a given world sheet described by $3m$ complex modular parameters.³ Here P_1 and P_2 are two points on the world-sheet. Since the field X , defining the embedding of the world-sheet into target space, is not a genuine conformal field of dimension zero, the Green function defined by eq. (2.1) depends on which local holomorphic coordinate system w_i we use at the point P_i , $i = 1, 2$.

³The ket-vacuum in (2.1) is the conformal one (i.e. a zero-momentum eigenstate), while the bra-vacuum is the state dual to this, i.e. a position eigenstate located at the origin.

We may introduce a single holomorphic coordinate z , given in terms of the local coordinate w_i by

$$w_i = V_i^{-1}(z) \quad \text{or} \quad z = V_i(w_i) . \quad (2.2)$$

It is conventional to take $w_i(P_i) = 0$. This implies that $z_i \equiv z(P_i) = V_i(0)$, $i = 1, 2$.

In terms of the coordinate z the Green function (2.1) may be written on the form [11]

$$G_{\text{str}}^{(m)}(z_1, z_2) = \ln \left| \frac{E(z_1, z_2)}{(V'_1(0)V'_2(0))^{1/2}} \right| - \frac{1}{2} \sum_{\mu, \nu=0}^m \Omega_\mu (2\pi \text{Im} \tau)^{-1}_{\mu\nu} \Omega_\nu , \quad (2.3)$$

where $E(z_1, z_2)$ is the prime form, τ is the period matrix and

$$\Omega_\mu = \text{Re} \int_{z_1}^{z_2} \omega_\mu , \quad \mu = 0, 1, \dots, m , \quad (2.4)$$

is the real part of the μ th abelian integral. (Our conventions are such that in a canonical homology basis $\{a_\mu, b_\mu | \mu = 0, 1, \dots, m\}$ we have $\oint_{a_\mu} \omega_\nu = 2\pi i \delta_{\mu\nu}$ and $\oint_{b_\mu} \omega_\nu = 2\pi i \tau_{\mu\nu}$.)

The dependence on the choice of local coordinates w_1 and w_2 enters through the quantities $V'_i(0)$ which appear because the prime form carries conformal dimension $-1/2$ with respect to both arguments. When the Green function is used to compute a physical string amplitude, the dependence on the local coordinates always drops out by virtue of the on-shell conditions for the external string states; but in the Green function *per se*, the dependence does not drop out. Therefore, before we can compare the string Green function (2.3), evaluated in a corner of moduli space corresponding to a given Φ^3 particle diagram, with the particle Green function pertaining to that diagram, we have to specify our choice of local coordinates.

2.1 Choosing the Local Coordinates

In general, the local coordinate w_i may be chosen to depend on all the moduli of the world-sheet, and even on the positions of the vertex operators representing external states. However, only a proper choice of local coordinate will give rise to a string Green function that reproduces the particle Green function, as in (1.1), in the corners of moduli space corresponding to Φ^3 particle diagrams. Our task is to find out which is the proper choice.

To this end it is useful to first consider the simplest example of all, where the world-sheet on which the two X -operators are inserted is just an infinite cylinder, representing a freely propagating string. In this case the particle diagram is an infinite line, parametrized by a Schwinger proper time τ , and the particle Green function is

$$G_B^{\text{line}}(\tau_1, \tau_2) = |\tau_1 - \tau_2| , \quad (2.5)$$

as can be seen for example by taking the limit $T \rightarrow \infty$ in the known expression for the particle Green function of a loop of total SPT length T , given by [4], [13]

$$G_B(\tau_1, \tau_2) = |\tau_1 - \tau_2| - \frac{(\tau_1 - \tau_2)^2}{T} . \quad (2.6)$$

In string theory, the Green function (2.3) reduces in the case of zero loops to

$$G_{\text{str}}^{\text{tree}}(z_1, z_2) = \ln \left| \frac{z_1 - z_2}{(V'_1(0)V'_2(0))^{1/2}} \right| . \quad (2.7)$$

In order to relate the two Green functions (2.7) and (2.5) we first have to establish the relation between the coordinates z_i and the SPTs τ_i .

In the customary parametrization of the cylinder, where the infinite future corresponds to $z = \infty$ and the infinite past to $z = 0$, we have $z = \exp\{t + i\sigma\}$, where t is the time-coordinate on the world-sheet and $\sigma \in [0; 2\pi]$ labels the points on the closed string at fixed time. The relation between SPT τ and the coordinate t can be found by requiring that the operator generating the time translation $t \rightarrow t' = t - \delta t$, which is given by $\delta t(L_0 + \bar{L}_0)$, assumes the standard form $\delta\tau(p^2 + m^2)$ when acting on any string state satisfying the level-matching condition $L_0 = \bar{L}_0 = \frac{\alpha'}{4}(p^2 + m^2)$. One finds

$$\tau = \frac{\alpha'}{2}t + \tau_0 = \frac{\alpha'}{2} \ln |z| + \tau_0 , \quad (2.8)$$

where τ_0 is an unspecified additive constant.

In a more general parametrization, where the infinite future and infinite past are represented by $z = z_\alpha$ and $z = z_\beta$ respectively, the relation (2.8) becomes

$$\tau = \frac{\alpha'}{2} \ln \left| \frac{z - z_\beta}{z - z_\alpha} \right| + \text{constant} = \frac{\alpha'}{2} \text{Re} \int^z \omega , \quad (2.9)$$

where

$$\omega(z) = \frac{1}{z - z_\beta} - \frac{1}{z - z_\alpha} = \frac{z_\beta - z_\alpha}{(z - z_\alpha)(z - z_\beta)} \quad (2.10)$$

is the *unique* holomorphic one-form on the cylinder satisfying the normalization condition

$$\int_a \omega = 2\pi i , \quad (2.11)$$

a being the homology cycle encircling the cylinder (represented in the z -plane by any curve encircling z_β but not z_α).

We now consider the proper choice of local coordinate. By definition

$$(V'_i(0))^{-1} = \left. \frac{dw_i}{dz} \right|_{z=z_i} \quad (2.12)$$

carries conformal dimension one with respect to z_i . This observation makes it very tempting to identify $(V'_i(0))^{-1}$ with the unique holomorphic one-form ω , evaluated at the point z_i , i.e. to take

$$V'_i(0) = (\omega(z_i))^{-1} = \frac{(z_i - z_\alpha)(z_i - z_\beta)}{z_\beta - z_\alpha} . \quad (2.13)$$

As we now proceed to show, this choice does indeed ensure that the string Green function (2.7) reduces to the particle Green function (2.5) in the field theory limit, as in (1.1). Choosing for simplicity the constant in eq. (2.9) to be zero, it follows that in the limit where $\alpha' \rightarrow 0$ for fixed τ , the point z must approach either z_α or z_β depending on whether τ is positive or negative. Since we are free to choose the location of $\tau = 0$, we may assume τ_1 and τ_2 to be positive without loss of generality, so that z_1 and z_2 both approach z_α .

In this limit

$$\tau_1 - \tau_2 = \frac{\alpha'}{2} \ln \left| \frac{z_1 - z_\beta}{z_1 - z_\alpha} \frac{z_2 - z_\alpha}{z_2 - z_\beta} \right| \simeq -\frac{\alpha'}{2} \ln \left| \frac{z_1 - z_\alpha}{z_2 - z_\alpha} \right| , \quad (2.14)$$

and we see that there are two orderings to consider, namely $\tau_1 > \tau_2$, corresponding to $|z_1 - z_\alpha| \ll |z_2 - z_\alpha|$, and $\tau_2 > \tau_1$, corresponding to $|z_2 - z_\alpha| \ll |z_1 - z_\alpha|$. In the first case we find

$$G_{\text{str}}^{\text{tree}}(z_1, z_2) \xrightarrow{\alpha' \rightarrow 0} \ln \left| \frac{z_2 - z_\alpha}{z_1 - z_\alpha} \right|^{1/2} = \frac{1}{\alpha'} (\tau_1 - \tau_2) , \quad (2.15)$$

and in the second case we obtain the same result, with labels 1 and 2 interchanged. In summary, we find the desired behaviour

$$G_{\text{str}}^{\text{tree}}(z_1, z_2) \xrightarrow{\alpha' \rightarrow 0} \frac{1}{\alpha'} |\tau_1 - \tau_2| = \frac{1}{\alpha'} G_B^{\text{line}}(\tau_1, \tau_2) , \quad (2.16)$$

regardless of the ordering chosen for the SPTs.

Our task is to generalize the prescription (2.13) to any world-sheet resembling a particle Φ^3 diagram. But how can ω be specified on a world-sheet containing several external legs and handles, where the holomorphic one-forms span a vector space of complex dimension greater than one? Fortunately, for the degenerate world-sheets resembling Φ^3 vacuum diagrams there is an essentially unique way to do this: Any vacuum Φ^3 diagram consists of propagators joined together at 3-point vertices. Any propagator having a fixed SPT length corresponds to a cylinder that becomes infinitely long (in units of the diameter) in the limit $\alpha' \rightarrow 0$. As we have seen, there is a *unique* one-form ω that is holomorphic at all points of an infinitely long cylinder and satisfies the normalization condition (2.11). Therefore, our prescription for choosing $V'_i(0)$ for a world-sheet resembling a given Φ^3 -diagram, with the point z_i sitting on some very long cylinder corresponding to an internal propagator of the vacuum diagram, is simply to take

$$V'_i(0) = (\omega(z_i))^{-1} , \quad (2.17)$$

where ω is *any* one-form that is: i) holomorphic at all points of the cylinder on which the point z_i is located; and ii) satisfies the normalization condition (2.11), a being a closed contour encircling the cylinder. In the limit $\alpha' \rightarrow 0$, where the cylinder becomes infinitely long, all such choices will be equivalent.

2.2 Identifying the Proper Pinching Limit

In this subsection we show how to identify a pinching limit (i.e. a corner of moduli space) where the string world-sheet degenerates into any given N-point $(m + 1)$ -loop Φ^3 particle diagram. Of course, for the analysis of the Green function we only need the

case $N = 2$, but since the generalization to arbitrary N does not present any further complications, we may as well be general.

As explained in more detail in refs. [14],[10], the relevant pinching limit can be identified by carefully constructing the degenerate world-sheet using the sewing procedure of refs. [11],[15]. In this paper we formulate a recipe which allows one to identify the pinching limit corresponding to a given diagram without having to go into the subtleties of the sewing procedure.

To be specific, we need a concrete parametrization of moduli space. The Schottky parametrization [12] of Riemann surfaces turns out to be very useful for our purposes. In this parametrization, the world-sheet of the string is described as a sphere with $m + 1$ pairs of holes, and each pair of holes is connected by a tube, thus forming a handle. The positions of the two holes forming the μ th pair is parametrized by points z_{α_μ} and z_{β_μ} in the compactified complex plane $\mathbf{C} \cup \{\infty\}$, and the length of the closed loop that we form by the insertion of the connecting tube is described by the modulus of a complex parameter k_μ , known as a *multiplier*.

The relation between the multiplier k_μ and the *total* Schwinger proper time T_μ of the μ th closed loop, formed by joining together the μ th pair of holes, is given by

$$T_\mu = -\frac{\alpha'}{2} \ln |k_\mu| , \quad (2.18)$$

and in the particle limit, where we take $\alpha' \rightarrow 0$ while keeping T_μ fixed, all multipliers become infinitely small

$$k_\mu \rightarrow 0 \quad , \quad \mu = 0, 1, \dots, m . \quad (2.19)$$

When all the multipliers are approaching zero, the various quantities defining the Green function (2.3) assume the following simple form

$$E(z_1, z_2) = z_1 - z_2 + \mathcal{O}(k_\mu) , \quad (2.20)$$

$$(2\pi \text{Im}\tau)_{\mu\nu} = -\delta_{\mu\nu} \ln |k_\mu| - (1 - \delta_{\mu\nu}) \ln \left| \frac{z_{\alpha_\mu} - z_{\alpha_\nu}}{z_{\alpha_\mu} - z_{\beta_\nu}} \frac{z_{\beta_\mu} - z_{\beta_\nu}}{z_{\beta_\mu} - z_{\alpha_\nu}} \right| + \mathcal{O}(k_\mu, \bar{k}_\mu) , \quad (2.21)$$

$$\Omega_\mu = \ln \left| \frac{z_2 - z_{\beta_\mu}}{z_1 - z_{\beta_\mu}} \frac{z_1 - z_{\alpha_\mu}}{z_2 - z_{\alpha_\mu}} \right| + \mathcal{O}(k_\mu, \bar{k}_\mu) . \quad (2.22)$$

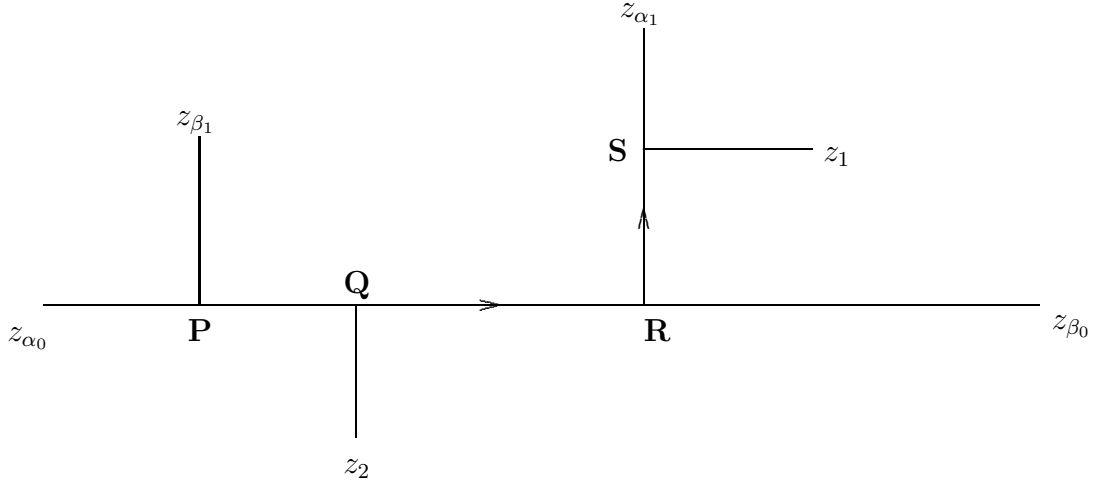


Figure 1: Example of a tree with one side-branch. The branch endpoints are $z_{B_0} = z_{\beta_0}$ and $z_{B_1} = z_{\alpha_1}$. The vertices P, Q, R and S are labelled by $z_{\beta_1}, z_2, z_{\alpha_1}$ and z_1 respectively.

However, to fully define the pinching limit corresponding to a given N -point $(m+1)$ -loop Φ^3 particle diagram, just taking the multipliers to be very small does not suffice. We still have to specify the behaviour of the $2m+N+2$ points z_i , $i = 1, \dots, N$ and $z_{\alpha_\mu}, z_{\beta_\mu}$, $\mu = 0, 1, \dots, m$. This we do as follows: First we cut open all the loops of the diagram so as to form a $2m+2+N$ -point Φ^3 tree diagram, \mathcal{T} , where the original external legs are labelled by z_i , $i = 1, \dots, N$ and the pair of external legs formed by cutting the μ th loop by z_{α_μ} and z_{β_μ} , $\mu = 0, 1, \dots, m$ (for example, see Fig.1). Projective invariance allows us to fix, say, $z_{\alpha_0} = \infty$ and $z_{\beta_0} = 0$.⁴ Then the remaining $2m+N$ external legs, which we call the *movable external legs*, are labelled by the points z_i , $i = 1, \dots, N$ and $z_{\alpha_j}, z_{\beta_j}$, $j = 1, \dots, m$, and we want to specify how to pinch these points. To this end it is very helpful to think of some flow of SPT, τ , starting at the leg labelled by $z_{\alpha_0} = \infty$ and flowing towards the future. We follow the flow all the way to the future endpoint which we take to be at the leg labelled by $z_{\beta_0} = 0$. This defines what we call the *main*

⁴We could actually fix the position of a third point, but we prefer not to do so.

branch, B_0 , of the tree diagram \mathcal{T} . The endpoint of the branch B_0 we also denote by z_{B_0} , i.e. $z_{B_0} = z_{\beta_0}$. In general not all the remaining external legs will be inserted as stems on the main branch; instead the diagram will have one or more *side-branches* B_1, B_2, \dots . Each side-branch B_i has its own flow of SPT, $\tau^{(i)}$, which we take to begin (with the value $\tau^{(i)} = 0$) at the vertex where the side-branch is joined to the main branch. Now, the side-branch B_i ends with *two* external legs, and so we choose one of them to represent the endpoint, z_{B_i} , of the side-branch B_i , and of the SPT flow $\tau^{(i)}$, and the other is then considered to be a stem inserted on the side-branch.

In exactly the same way, the side-branches may themselves have side-branches, which give rise to new SPT flows. At the end we have decomposed the entire tree diagram into the main branch B_0 and a set of side-branches B_i , $i = 1, \dots, N_b$, each having its own SPT flow. The direction of the SPT flow $\tau^{(i)}$ (towards the endpoint z_{B_i}) defines a SPT ordering of the vertices along the branch B_i .

Furthermore, the $2m + N$ movable external legs have been divided into side-branch endpoints z_{B_i} , $i = 1, \dots, N_b$, and stems inserted on the branches. Keeping this in mind we may now establish a one-to-one correspondence between the vertices of the diagram and the points $z_1, \dots, z_N; z_{\alpha_1}, z_{\beta_1}, \dots, z_{\alpha_m}, z_{\beta_m}$ labelling the movable external legs. Simply, if $z \in \{z_1, \dots, z_N; z_{\alpha_1}, z_{\beta_1}, \dots, z_{\alpha_m}, z_{\beta_m}\}$ labels a stem inserted on a branch, then z is associated with the corresponding vertex. Instead, if z labels a side-branch endpoint, then z is associated with the vertex at which the side-branch is attached. An example is shown in Fig.1.

The pinching limit corresponding to the given diagram is now identified as follows: The z -values associated to the vertices of the branch B_i , $i = 0, 1, \dots, N_b$, all approach the branch endpoint z_{B_i} , i.e.

$$|z - z_{B_i}| \ll 1 . \quad (2.23)$$

Furthermore, z -values associated to vertices having “late” values of $\tau^{(i)}$ approach z_{B_i} much faster than z -values associated to vertices having “early” values of $\tau^{(i)}$. Thus, if z and \tilde{z} are associated with two vertices along the branch B_i , having SPTs $\tau^{(i)}$ and $\tilde{\tau}^{(i)}$

respectively, then

$$\begin{aligned} |z - z_{B_i}| \ll |\tilde{z} - z_{B_i}| \ll 1 & \text{ if } \tau^{(i)} > \tilde{\tau}^{(i)} \\ |\tilde{z} - z_{B_i}| \ll |z - z_{B_i}| \ll 1 & \text{ if } \tilde{\tau}^{(i)} > \tau^{(i)}. \end{aligned} \quad (2.24)$$

One should note that in general there will be many different pinching limits that give rise to the same Φ^3 -diagram. For example, the pinching limit that we obtain by interchanging z_{α_μ} and z_{β_μ} will rather obviously define the same diagram – after all, when we form two external legs by cutting open the μ th loop, it is a matter of pure convention which one is labelled by z_{α_μ} and which one by z_{β_μ} . Similarly, any pinching limit that is obtained by permuting the m triplets $\{k_j, z_{\alpha_j}, z_{\beta_j}\}$ will also correspond to the same Φ^3 -diagram, since one is just changing the numbering of the loops.

The existence of several equivalent pinching limits merely reflects the fact that we are working in Teichmüller space: The equivalent pinching limits are related by modular transformations and correspond to the same corner of moduli space. One is therefore free to choose any one of the equivalent pinching limits to represent the corner of moduli space corresponding to a given Φ^3 -diagram.

In section 4 we provide some explicit examples that may help to clarify the general procedure for identifying a pinching limit that we have given in this section.

2.3 The Mapping of String Moduli into SPT

In the previous subsection we already introduced a SPT parametrization of any given Φ^3 particle diagram: Along the main branch we use the SPT $\tau \equiv \tau^{(0)}$, flowing from z_{α_0} towards z_{β_0} , and along the side-branch B_i we define the SPT $\tau^{(i)}$, starting at zero value at the vertex where the side-branch is attached to the main part of the tree and flowing towards the endpoint z_{B_i} . We also identified a pinching limit describing the corner in string moduli space where the world-sheet degenerates into the particle diagram.

In this subsection we present the precise mapping between the points of the set $M \equiv \{z_1, \dots, z_N; z_{\alpha_1}, z_{\beta_1}, \dots, z_{\alpha_m}, z_{\beta_m}\}$ and the SPTs of the vertices in the particle diagram. Remember that to each vertex we have associated a point $z \in M$. Then, if two vertices

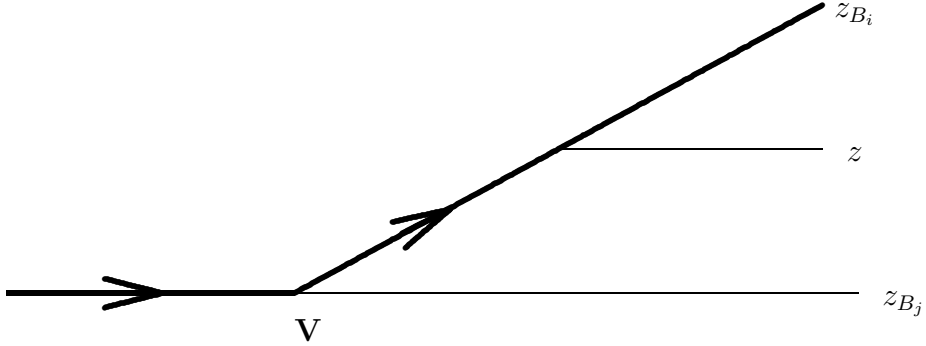


Figure 2: How to obtain eq. (2.27). The thick line represents the new SPT flow. See the text for details.

belonging to the branch B_i have SPTs $\tau^{(i)}$ and $\tilde{\tau}^{(i)}$ and are associated to the points z and \tilde{z} respectively, the relation, like in eq. (2.14), is simply given by

$$\tau^{(i)} - \tilde{\tau}^{(i)} = -\frac{\alpha'}{2} \ln \left| \frac{z - z_{B_i}}{\tilde{z} - z_{B_i}} \right| . \quad (2.25)$$

It is clear that with this precise identification, the pinching limit (2.24) amounts to the statement that $|\tau^{(i)} - \tilde{\tau}^{(i)}|/\alpha' \gg 1$, i.e. that the cylinder connecting the two vertices is very long in string units. As we recall, the formal field theory limit is obtained by taking $\alpha' \rightarrow 0$ for fixed SPT values.

The expression (2.25) only defines *differences* of SPT values along the branch B_i . It does not provide the relation between the points of the set M and the SPT of a single vertex. For vertices along the main branch B_0 , we simply take

$$\tau = -\frac{\alpha'}{2} \ln |z| , \quad (2.26)$$

while for vertices along the side-branch B_i , $i = 1, \dots, N_b$, the relation is

$$\tau^{(i)} = -\frac{\alpha'}{2} \ln \left| \frac{z - z_{B_i}}{z_{B_j} - z_{B_i}} \right| , \quad (2.27)$$

where B_j , $j \in \{0, 1, \dots, i-1, i+1, \dots, N_b\}$, is the branch to which B_i is attached. To derive eq. (2.27) we may refer back to the sewing procedure [11],[15], but the following argument is easier (see Fig.2): We consider the side-branch B_i to be attached to the

branch B_j at the vertex V , and according to this decomposition of the tree into branches, the SPT flow $\tau^{(i)}$ starts at the vertex V . Now, the vertex V divides the branch B_j into two: speaking in terms of the SPT flow $\tau^{(j)}$ these are the parts of the branch B_j happening “before” and “after” the vertex. This division allows us to define a new decomposition of the tree diagram into branches, one where we consider the part of the old branch B_j happening *after* the vertex V to be a side-branch inserted on the branch formed by combining the part of the old branch B_j happening *before* the vertex with the old side-branch B_i . Corresponding to this new decomposition of the diagram into branches, we have a new SPT, $\tau_{\text{new}}^{(i)}$, which is zero at the point of the diagram where the old SPT $\tau^{(j)}$ was zero, but which still runs towards the point z_{B_i} . Furthermore, with the new decomposition, both the vertex V , which according to our rules is now associated with the point z_{B_j} , as well as the vertex associated with the point z , now belong to the branch B_i , and therefore we may use eq. (2.25) to compute the SPT interval $\Delta\tau_{\text{new}}^{(i)}$ between the two vertices. Since by definition this interval is nothing but the value taken by the old SPT $\tau^{(i)}$ at the vertex associated with z , we arrive at the expression (2.27).

Since $\tau^{(i)}$ is positive and very large in units of α' , the relation (2.27) implies that the pinching limit (2.23) is further specified by the inequality

$$|z - z_{B_i}| \ll |z_{B_j} - z_{B_i}| . \quad (2.28)$$

3 The Green Function in Particle Theory

Schmidt and Schubert have obtained the bosonic worldline Green function for the class of multi-loop diagrams where all vertices are located on a single fundamental loop. Their Green function was originally derived in the scalar Φ^3 theory [6] and was subsequently applied to a specific type of multiloop photon diagrams in spinor QED [7]. In the worldline formulation of Φ^3 theory, the sum of all N -point $(m + 1)$ -loop Feynman diagrams that have their vertices located on a single loop is expressed by the following integral over

SPTs (omitting for simplicity the coupling constant and mass factors):

$$\begin{aligned}\Gamma_N^{(m+1)} &= \int_0^\infty \frac{dT}{T} T^{-D/2} (4\pi)^{-\frac{D}{2}(m+1)} \prod_{i=1}^m \int_0^\infty d\bar{T}_i \int_0^T d\tau_{\alpha_i} \int_0^T d\tau_{\beta_i} \prod_{n=1}^N \int_0^T d\tau_n \\ &\times (\det A)^{-D/2} \exp\left[\frac{1}{2} \sum_{k,l=1}^N p_k p_l G_B^{(m)}(\tau_k, \tau_l)\right].\end{aligned}\quad (3.1)$$

Here all points on the fundamental loop are labelled by a SPT $\tau \in [0; T]$. Thus, τ_1, \dots, τ_N are the points where the external legs have been inserted and the extra loops have been obtained by joining together the points $\tau = \tau_{\alpha_i}$ and $\tau = \tau_{\beta_i}$ by means of an internal propagator of SPT length \bar{T}_i , $i = 1, \dots, m$. The worldline Green function is given by

$$\begin{aligned}G_B^{(m)}(\tau_1, \tau_2) &= \\ G_B(\tau_1, \tau_2) &+ \frac{1}{2} \sum_{i,j=1}^m [G_B(\tau_1, \tau_{\alpha_i}) - G_B(\tau_1, \tau_{\beta_i})] A_{ij}^{-1} [G_B(\tau_2, \tau_{\alpha_j}) - G_B(\tau_2, \tau_{\beta_j})],\end{aligned}\quad (3.2)$$

where A is the symmetric $m \times m$ matrix defined by ⁵

$$A_{ij} \equiv \bar{T}_i \delta_{ij} - X(\tau_{\alpha_i}, \tau_{\beta_i}; \tau_{\alpha_j}, \tau_{\beta_j}), \quad (3.3)$$

$$X(\tau_a, \tau_b; \tau_c, \tau_d) \equiv \frac{1}{2} [G_B(\tau_a, \tau_c) - G_B(\tau_a, \tau_d) - G_B(\tau_b, \tau_c) + G_B(\tau_b, \tau_d)]. \quad (3.4)$$

In these formulae G_B is the one-loop Green function given by eq. (2.6).

Actually, what we obtain from the string Green function by taking the field theory limit is not $G_B^{(m)}$, but rather the redefined Green function

$$\tilde{G}_B^{(m)}(\tau_1, \tau_2) = G_B^{(m)}(\tau_1, \tau_2) - \frac{1}{2} G_B^{(m)}(\tau_1, \tau_1) - \frac{1}{2} G_B^{(m)}(\tau_2, \tau_2), \quad (3.5)$$

which by construction satisfies $\tilde{G}_B^{(m)}(\tau, \tau) = 0$. In eq. (3.1) we can replace $G_B^{(m)}$ by $\tilde{G}_B^{(m)}$, since the extra terms in the exponent cancel due to conservation of the external momenta.

By using eq. (3.2) we find

$$\tilde{G}_B^{(m)}(\tau_1, \tau_2) = G_B(\tau_1, \tau_2) - \sum_{i,j=1}^m X(\tau_1, \tau_2; \tau_{\alpha_i}, \tau_{\beta_i}) A_{ij}^{-1} X(\tau_1, \tau_2; \tau_{\alpha_j}, \tau_{\beta_j}). \quad (3.6)$$

⁵Notice that our matrix A is the inverse of the matrix A used in refs. [6],[7].

Other types of Green functions appear if we want to consider the situation where external legs are inserted not only on the fundamental loop but also on the internal propagators. These Green functions can be obtained by a straightforward generalization of the path-integral derivation leading to the expression (3.1). This expression was obtained by Schmidt and Schubert by computing an open path integral $\mathcal{D}x^{(i)}$, $i = 1, \dots, m$ for each internal propagator and finally a closed path integral $\mathcal{D}x$ for the fundamental loop, with the insertion of N vertex operators (see ref. [6] for details)

$$\int_0^T d\tau_n \exp[i p_n x(\tau_n)] , \quad n = 1, \dots, N , \quad (3.7)$$

corresponding to the source

$$J(\tau) = i \sum_{n=1}^N p_n \delta(\tau - \tau_n) . \quad (3.8)$$

To obtain the other types of Green functions we imagine inserting vertex operators

$$\int_0^{\bar{T}_j} d\tau_n^{(j)} \exp[i p_n^{(j)} x^{(i)}(\tau_n^{(j)})] , \quad n = 1, \dots, N_j , \quad (3.9)$$

into the open path integral pertaining to the j 'th internal propagator, $j = 1, 2, \dots, m$ (total number of external legs is now $N = N_L + \sum N_i$). This obviously modifies the result of computing the open path integrals, giving rise to a more complicated source

$$J(\tau) = i \sum_{n=1}^{N_L} p_n \delta(\tau - \tau_n) + i \sum_{i=1}^m \sum_{n=1}^{N_i} p_n^{(i)} \left[\delta(\tau - \tau_{\alpha_i}) + \frac{\tau_n^{(i)}}{\bar{T}_i} \{ \delta(\tau - \tau_{\beta_i}) - \delta(\tau - \tau_{\alpha_i}) \} \right] , \quad (3.10)$$

as well as an additional exponential factor $\exp(I)$, where

$$I = \frac{1}{2} \sum_{i=1}^m \sum_{n,n'=1}^{N_i} p_n^{(i)} p_{n'}^{(i)} \{ |\tau_n^{(i)} - \tau_{n'}^{(i)}| - \tau_n^{(i)} - \tau_{n'}^{(i)} + \frac{2\tau_n^{(i)}\tau_{n'}^{(i)}}{\bar{T}_i} \} . \quad (3.11)$$

Finally, performing the path integral for the fundamental loop, one obtains the following exponential factor from which the Green functions can be read

$$\begin{aligned} \exp(I) \exp \left[-\frac{1}{2} \int_0^T d\tau d\tau' J(\tau) G_B^{(m)}(\tau, \tau') J(\tau') \right] \equiv \\ \exp \left[\frac{1}{2} \sum_{i,j=0}^m \sum_{n=1}^{N_i} \sum_{n'=1}^{N_j} p_n^{(i)} p_{n'}^{(j)} G_{ij}^{(m)}(\tau_n^{(i)}, \tau_{n'}^{(j)}) \right] . \end{aligned} \quad (3.12)$$

(Here we introduced the convenient and rather obvious notation $\tau_n^{(0)} \equiv \tau_n$ and $p_n^{(0)} \equiv p_n$, $n = 1, \dots, N_L \equiv N_0$). After some rearrangement similar to (3.5), using conservation of external momentum to obtain $G_{ii}^{(m)}(\tau^{(i)}, \tau^{(i)}) = 0$ for $i = 0, 1, \dots, m$, we find

$$G_{00}^{(m)}(\tau_1, \tau_2) = \tilde{G}_B^{(m)}(\tau_1, \tau_2), \quad (3.13)$$

$$G_{ii}^{(m)}(\tau_1^{(i)}, \tau_2^{(i)}) = |\tau_1^{(i)} - \tau_2^{(i)}| - \frac{(\tau_1^{(i)} - \tau_2^{(i)})^2}{\bar{T}_i} (1 + \frac{1}{\bar{T}_i} X_{ii}^{(m)}), \quad (3.14)$$

$$G_{i0}^{(m)}(\tau_1^{(i)}, \tau_2) = \tau_1^{(i)} + \tilde{G}_B^{(m)}(\tau_{\alpha_i}, \tau_2) - \frac{\tau_1^{(i)2}}{\bar{T}_i} (1 + \frac{1}{\bar{T}_i} X_{ii}^{(m)}) + 2 \frac{\tau_1^{(i)}}{\bar{T}_i} X^{(m)}(\tau_{\alpha_i}, \tau_2; \tau_{\alpha_i}, \tau_{\beta_i}), \quad (3.15)$$

$$\begin{aligned} G_{ij}^{(m)}(\tau_1^{(i)}, \tau_2^{(j)}) &= \tau_1^{(i)} + \frac{1}{2} \tilde{G}_B^{(m)}(\tau_{\alpha_i}, \tau_{\alpha_j}) - \frac{\tau_1^{(i)2}}{\bar{T}_i} (1 + \frac{1}{\bar{T}_i} X_{ii}^{(m)}) \\ &+ \frac{\tau_1^{(i)} \tau_2^{(j)}}{\bar{T}_i \bar{T}_j} X_{ij}^{(m)} + 2 \frac{\tau_1^{(i)}}{\bar{T}_i} X^{(m)}(\tau_{\alpha_i}, \tau_{\alpha_j}; \tau_{\alpha_i}, \tau_{\beta_i}) + (1, i \leftrightarrow 2, j \text{ for all terms}), \end{aligned} \quad (3.16)$$

where, in analogy with eq. (3.4), we have defined

$$\begin{aligned} X^{(m)}(\tau_a, \tau_b; \tau_c, \tau_d) &\equiv \\ \frac{1}{2} \left[G_B^{(m)}(\tau_a, \tau_c) - G_B^{(m)}(\tau_a, \tau_d) - G_B^{(m)}(\tau_b, \tau_c) + G_B^{(m)}(\tau_b, \tau_d) \right] &, \end{aligned} \quad (3.17)$$

and we also introduced the notation

$$X_{ij}^{(m)} \equiv X^{(m)}(\tau_{\alpha_i}, \tau_{\beta_i}; \tau_{\alpha_j}, \tau_{\beta_j}) \quad \text{and} \quad X_{ij} \equiv X(\tau_{\alpha_i}, \tau_{\beta_i}; \tau_{\alpha_j}, \tau_{\beta_j}). \quad (3.18)$$

Here the convention is that the SPT $\tau^{(i)}$ starts at zero value at the vertex $\tau = \tau_{\alpha_i}$ and ends (at value \bar{T}_i) at the vertex $\tau = \tau_{\beta_i}$. Eqs.(3.14) and (3.15) are obtained in ref. [16] in the $m = 1$ case.

In the Appendix we prove the following two identities:

$$A_{ij}^{-1} = \frac{1}{\bar{T}_i \bar{T}_j} (\bar{T}_i \delta_{ij} + X_{ij}^{(m)}), \quad (3.19)$$

$$\sum_{k=1}^m A_{ik}^{-1} X(\tau_a, \tau_b; \tau_{\alpha_k}, \tau_{\beta_k}) = \frac{1}{\bar{T}_i} X^{(m)}(\tau_a, \tau_b; \tau_{\alpha_i}, \tau_{\beta_i}), \quad (3.20)$$

and by using these, together with eq. (3.6), we can rewrite the Green functions (3.14) - (3.16) on a more compact form:

$$G_{ii}^{(m)}(\tau_1^{(i)}, \tau_2^{(i)}) = |\tau_1^{(i)} - \tau_2^{(i)}| - (\tau_1^{(i)} - \tau_2^{(i)})^2 A_{ii}^{-1}, \quad (3.21)$$

$$\begin{aligned}
G_{i0}^{(m)}(\tau_1^{(i)}, \tau_2) &= \tau_1^{(i)} + G_B(\tau_{\alpha_i}, \tau_2) \\
&\quad - \sum_{k,l=1}^m [-\tau_1^{(i)} \delta_{ik} + X_k(\tau_{\alpha_i}, \tau_2)] A_{kl}^{-1} [-\tau_1^{(i)} \delta_{il} + X_l(\tau_{\alpha_i}, \tau_2)], \quad (3.22)
\end{aligned}$$

$$\begin{aligned}
G_{ij}^{(m)}(\tau_1^{(i)}, \tau_2^{(j)}) &= \tau_1^{(i)} + \tau_2^{(j)} + G_B(\tau_{\alpha_i}, \tau_{\alpha_j}) \\
&\quad - \sum_{k,l=1}^m [-\tau_1^{(i)} \delta_{ik} + \tau_2^{(j)} \delta_{jk} + X_k(\tau_{\alpha_i}, \tau_{\alpha_j})] A_{kl}^{-1} [-\tau_1^{(i)} \delta_{il} + \tau_2^{(j)} \delta_{jl} + X_l(\tau_{\alpha_i}, \tau_{\alpha_j})], \quad (3.23)
\end{aligned}$$

where we introduced the shorthand notation

$$X_j(\tau_a, \tau_b) \equiv X(\tau_a, \tau_b; \tau_{\alpha_j}, \tau_{\beta_j}). \quad (3.24)$$

In the following section we will show how the string Green function reduces, in the relevant field theory limit, to the Green functions (3.6),(3.21),(3.22) and (3.23).

4 Reducing String Theory to Particle Theory

In this section we show how the string Green function, supplemented with our prescribed choice of local coordinates, correctly reproduces the particle theory Green functions (3.6),(3.21),(3.22) and (3.23) in the respective field theory limits.

The Green functions $G_{\mu\nu}^{(m)}$ correspond to different (classes of) Φ^3 -diagrams, depending on the values taken by $\mu, \nu \in \{0, 1, \dots, m\}$, and as explained in section 2 these different classes of diagrams correspond to different (classes of) corners of string moduli space, hence to different classes of pinching limits. But before we enter into the details of individual pinching limits, it is advantageous to rewrite the string Green function (2.3) on a form more similar to the world-line Green functions. As it stands, the string formula involves the period matrix, which is an $(m+1) \times (m+1)$ -matrix, whereas the world-line formulae involve the $m \times m$ -matrix A and are expressed in terms of the one-loop Green function.

To mimic the world-line formulation, where the particle diagram is constructed from a fundamental loop with total Schwinger proper time T , we single out the string loop

labelled by $\mu = 0$ and make the identification (as in eq. (2.18))

$$T = -\frac{\alpha'}{2} \ln |k_0| = \frac{\alpha'}{2} (2\pi \text{Im}\tau)_{00} \equiv \frac{\alpha'}{2} \Delta . \quad (4.1)$$

Our task is then to reexpress the $(m+1)$ -loop Green function given by eq. (2.3), in terms of the one-loop Green function obtained by setting $m = 0$ in eq. (2.3). In our standard configuration

$$z_{\alpha_0} = \infty, \quad z_{\beta_0} = 0 , \quad (4.2)$$

we find

$$G_{\text{str}}^{(0)}(z_1, z_2) = \ln \left| \frac{z_1 - z_2}{z_1^{1/2} z_2^{1/2}} \right| - \frac{1}{2\Delta} \ln^2 \left| \frac{z_2}{z_1} \right| + \mathcal{O}(k_\mu, \bar{k}_\mu) . \quad (4.3)$$

Here we used our choice (2.13) of the local coordinate, which for the case of a torus in the standard configuration (4.2) is reduced to

$$V'_i(0) = z_i . \quad (4.4)$$

This coincides with the choice made in ref. [17].

We now turn our attention to the $(m+1)$ -loop Green function given by eq. (2.3). As a first step we may rewrite it as follows ⁶

$$\begin{aligned} G_{\text{str}}^{(m)}(z_1, z_2) &= \ln \left| \frac{z_1^{1/2} z_2^{1/2}}{(V'_1(0))^{1/2} (V'_2(0))^{1/2}} \right| + G_{\text{str}}^{(0)}(z_1, z_2) \\ &+ \frac{1}{2} (\Omega_0)^2 \left[\frac{1}{\Delta} - (2\pi \text{Im}\tau)_{00}^{-1} \right] - \frac{1}{2} \sum_{i,j=1}^m \Omega_i \Omega_j (2\pi \text{Im}\tau)_{ij}^{-1} - \Omega_0 \sum_{i=1}^m \Omega_i (2\pi \text{Im}\tau)_{0i}^{-1} , \end{aligned} \quad (4.5)$$

where we used eq. (4.3).

In eq. (4.5) the quantities $V'_i(0)$ refer to the choice of local coordinates on the genus $m+1$ Riemann surface and as such will be chosen differently in the various corners of moduli space, as explained in subsection 2.1.

Now, since the matrix (2.21) satisfies the obvious identity

$$\sum_{\mu=0}^m (2\pi \text{Im}\tau)_{0\mu} (2\pi \text{Im}\tau)_{\mu\nu}^{-1} = \Delta (2\pi \text{Im}\tau)_{0\nu}^{-1} + \sum_{i=1}^m x_i (2\pi \text{Im}\tau)_{i\nu}^{-1} = \delta_{0\nu} , \quad (4.6)$$

⁶ From now on we will stop writing explicitly the $\mathcal{O}(k_\mu)$ terms, with the understanding that everything holds only in the limit of vanishing multipliers.

where we defined

$$x_i \equiv \ln \left| \frac{z_{\alpha_i}}{z_{\beta_i}} \right| = (2\pi \text{Im}\tau)_{0i} , \quad (4.7)$$

we can rewrite the 3rd and 5th terms on the r.h.s. of eq. (4.5) as follows;

$$(2\pi \text{Im}\tau)_{0i}^{-1} = - \sum_{j=1}^m x_j \Delta^{-1} (2\pi \text{Im}\tau)_{ij}^{-1} , \quad (4.8)$$

$$\frac{1}{\Delta} - (2\pi \text{Im}\tau)_{00}^{-1} = \sum_{i=1}^m x_i \Delta^{-1} (2\pi \text{Im}\tau)_{i0}^{-1} = - \sum_{i,j=1}^m x_i x_j \Delta^{-2} (2\pi \text{Im}\tau)_{ij}^{-1} , \quad (4.9)$$

and thereby obtain

$$\begin{aligned} G_{\text{str}}^{(m)}(z_1, z_2) &= \ln \left| \frac{z_1^{1/2} z_2^{1/2}}{(V'_1(0))^{1/2} (V'_2(0))^{1/2}} \right| + G_{\text{str}}^{(0)}(z_1, z_2) \\ &\quad - \frac{1}{2} \Delta^{-2} \sum_{i,j=1}^m (\Delta \Omega_i - x_i \Omega_0) (\Delta \Omega_j - x_j \Omega_0) (2\pi \text{Im}\tau)_{ij}^{-1} . \end{aligned} \quad (4.10)$$

It is straightforward to verify that

$$\begin{aligned} X_{\text{str}}(z_1, z_2; z_{\alpha_i}, z_{\beta_i}) &\equiv G_{\text{str}}^{(0)}(z_1, z_{\alpha_i}) - G_{\text{str}}^{(0)}(z_1, z_{\beta_i}) - G_{\text{str}}^{(0)}(z_2, z_{\alpha_i}) + G_{\text{str}}^{(0)}(z_2, z_{\beta_i}) \\ &= \ln \left| \frac{z_2 - z_{\beta_i}}{z_1 - z_{\beta_i}} \frac{z_1 - z_{\alpha_i}}{z_2 - z_{\alpha_i}} \right| + \ln \left| \frac{z_{\alpha_i}}{z_{\beta_i}} \right| \ln \left| \frac{z_1}{z_2} \right| \Delta^{-1} \\ &= \Omega_i - x_i \Omega_0 \Delta^{-1} . \end{aligned} \quad (4.11)$$

Furthermore, the $m \times m$ matrix defined by

$$A_{ij}^{\text{str}} \equiv (2\pi \text{Im}\tau)_{ij} - x_i x_j \Delta^{-1} ; \quad i, j = 1, \dots, m , \quad (4.12)$$

is the inverse of the matrix $\{(2\pi \text{Im}\tau)_{ij}^{-1}\}_{i,j=1,\dots,m}$, i.e. satisfies

$$\sum_{k=1}^m A_{ik}^{\text{str}} (2\pi \text{Im}\tau)_{kj}^{-1} = \sum_{k=1}^m (2\pi \text{Im}\tau)_{ik}^{-1} A_{kj}^{\text{str}} = \delta_{ij} , \quad (4.13)$$

as can be seen by inspection, using eq. (4.8). By using eq. (4.11), replacing z_1 and z_2 with z_{α_j} and z_{β_j} respectively, we immediately find

$$A_{ij}^{\text{str}} = -X_{\text{str}}(z_{\alpha_i}, z_{\beta_i}; z_{\alpha_j}, z_{\beta_j}) \quad \text{for } i \neq j , \quad (4.14)$$

while for $i = j$ we have

$$A_{ii}^{\text{str}} = -\ln |k_i| - \ln^2 \left| \frac{z_{\alpha_i}}{z_{\beta_i}} \right| \Delta^{-1} = \bar{\Delta}_i + 2G_{\text{str}}^{(0)}(z_{\alpha_i}, z_{\beta_i}) , \quad (4.15)$$

where we defined

$$\bar{\Delta}_i \equiv -\ln \left| k_i \frac{(z_{\alpha_i} - z_{\beta_i})^2}{z_{\alpha_i} z_{\beta_i}} \right|. \quad (4.16)$$

Collecting our results (4.11) and (4.13), the world-sheet Green function (4.10) can now be written on the form

$$\begin{aligned} G_{\text{str}}^{(m)}(z_1, z_2) &= \ln \left| \frac{z_1^{1/2} z_2^{1/2}}{(V'_1(0))^{1/2} (V'_2(0))^{1/2}} \right| + G_{\text{str}}^{(0)}(z_1, z_2) \\ &\quad - \frac{1}{2} \sum_{i,j=1}^m X_{\text{str}}(z_1, z_2; z_{\alpha_i}, z_{\beta_i}) X_{\text{str}}(z_1, z_2; z_{\alpha_j}, z_{\beta_j}) (A^{\text{str}})^{-1}_{ij}. \end{aligned} \quad (4.17)$$

We want to evaluate this expression in the pinching limits pertaining to the specific world-line Green functions $G_{00}^{(m)}$, $G_{ii}^{(m)}$, $G_{0i}^{(m)}$ and $G_{ij}^{(m)}$. As previously explained, each of these worldline Green functions corresponds to different ways of inserting two external legs in what is actually a whole class of $(m+1)$ -loop Φ^3 vacuum diagrams, namely any diagram that can be obtained by joining together $2m$ vertices located on a fundamental loop by means of m internal propagators. Different Φ^3 vacuum diagrams arise from choosing different orderings of the SPTs of the $2m$ vertices.

In the string formulation, the mapping of the parameters $z_{\alpha_i}, z_{\beta_i}$ into the local SPTs $\tau_{\alpha_i}, \tau_{\beta_i}$ is straightforward, following the rules of subsection 2.3:

$$\begin{aligned} \tau_{\alpha_i} &= -\frac{\alpha'}{2} \ln |z_{\alpha_i}| \quad \text{for } i = 1, \dots, m, \\ \tau_{\beta_i} &= -\frac{\alpha'}{2} \ln |z_{\beta_i}| \quad \text{for } i = 1, \dots, m. \end{aligned} \quad (4.18)$$

Different orderings of the local proper times imply different pinching limits for the parameters z_{α_i} and z_{β_i} . For example the ordering

$$\tau_{\alpha_1} < \tau_{\alpha_2} < \dots < \tau_{\alpha_m} < \tau_{\beta_m} < \dots < \tau_{\beta_1}$$

is equivalent to the pinching limit

$$|z_{\beta_1}| \ll \dots \ll |z_{\beta_m}| \ll |z_{\alpha_m}| \ll \dots \ll |z_{\alpha_1}|$$

in the limit $\alpha' \rightarrow 0$.

We can have $(2m)!$ different orderings of these local proper times, and therefore as many different pinching limits. To analyze the field theory limit case by case is possible (we did it), but very tedious. Fortunately, there is a much quicker way: The Green function, as written in eq. (4.17), is expressed solely in terms of the one-loop Green function (4.3), and it is therefore sufficient to consider the field theory limit of this quantity. It is easy to verify that for any two points z_a and z_b related to SPTs τ_a and τ_b by eq. (4.18) we have

$$G_{\text{str}}^{(0)}(z_a, z_b) \xrightarrow{\alpha' \rightarrow 0} \frac{1}{\alpha'} G_B(\tau_a, \tau_b) , \quad (4.19)$$

regardless of which one of the two possible orderings of τ_a and τ_b we happen to consider. The proof is closely analogous to the one given for the cylinder in subsection 2.1.

In view of the scaling behaviour (4.19) we see that for $i \neq j$

$$A_{ij}^{\text{str}} = -X_{\text{str}}(z_{\alpha_i}, z_{\beta_i}; z_{\alpha_j}, z_{\beta_j}) \xrightarrow{\alpha' \rightarrow 0} \quad (4.20)$$

$$\begin{aligned} -\frac{1}{\alpha'} \left(G_B(\tau_{\alpha_i}, \tau_{\alpha_j}) - G_B(\tau_{\alpha_i}, \tau_{\beta_j}) - G_B(\tau_{\beta_i}, \tau_{\alpha_j}) + G_B(\tau_{\beta_i}, \tau_{\beta_j}) \right) = \\ -\frac{2}{\alpha'} X(\tau_{\alpha_i}, \tau_{\beta_i}; \tau_{\alpha_j}, \tau_{\beta_j}) = \frac{2}{\alpha'} A_{ij} , \end{aligned} \quad (4.21)$$

where we used eqs. (4.14), (4.11), (3.4) and (3.3).

In the diagonal case $i = j$ we encounter the quantity $\bar{\Delta}_i$, defined by eq. (4.16), which has the following behaviour

$$\bar{\Delta}_i \xrightarrow{\alpha' \rightarrow 0} \frac{2}{\alpha'} (T_i - |\tau_{\alpha_i} - \tau_{\beta_i}|) = \frac{2}{\alpha'} \bar{T}_i . \quad (4.22)$$

Here we see the fact that T_i , defined by eq. (2.18), is the SPT of the entire loop formed by the insertion of the internal propagator, whereas \bar{T}_i is only the SPT of the internal propagator itself.

Using the behaviour (4.22) and (4.19) in eq. (4.15), we find

$$A_{ii}^{\text{str}} \xrightarrow{\alpha' \rightarrow 0} \frac{2}{\alpha'} (\bar{T}_i + G_B(\tau_{\alpha_i}, \tau_{\beta_i})) = \frac{2}{\alpha'} A_{ii} . \quad (4.23)$$

In summary we have the scaling relation

$$A_{ij}^{\text{str}} \xrightarrow{\alpha' \rightarrow 0} \frac{2}{\alpha'} A_{ij} \quad (4.24)$$

for off-diagonal as well as diagonal elements.

To investigate the scaling behaviour of the other quantities appearing in the string Green function (4.17) we need to specify the pinching limit for z_1 and z_2 ; i.e., we have to consider case by case the situations corresponding to the various particle Green functions.

4.1 The Green Function $G_{00}^{(m)}$

The simplest case is when both external legs are inserted on the fundamental loop (Fig.3). In this case the tree diagram obtained by cutting open all the loops consists only of one (main) branch and the mapping into SPTs is given by eq. (2.26), i.e.

$$\tau_i = -\frac{\alpha'}{2} \ln |z_i| \quad \text{for } i = 1, 2 . \quad (4.25)$$

Thus the scaling behaviour (4.19) also holds for Green functions having z_1 and/or z_2 as argument. Accordingly

$$\begin{aligned} G_{\text{str}}^{(0)}(z_1, z_2) &\xrightarrow{\alpha' \rightarrow 0} \frac{1}{\alpha'} G_B(\tau_1, \tau_2) \\ X_{\text{str}}(z_1, z_2; z_{\alpha_i}, z_{\beta_i}) &\xrightarrow{\alpha' \rightarrow 0} \frac{2}{\alpha'} X(\tau_1, \tau_2; \tau_{\alpha_i}, \tau_{\beta_i}) . \end{aligned} \quad (4.26)$$

Finally, for $V'_i(0)$ we should use eq. (2.17) where for ω we may use any one of the holomorphic one-forms that satisfies the normalization condition (2.11). The homology cycle a is represented in the complex plane by a contour that encircles $z_{\beta_0} = 0$ as well as all those points z_{α_j} and z_{β_j} that label vertices with SPT values larger than τ_i . Thus, if we consider the standard basis of holomorphic one-forms, where

$$\omega_\mu(z) = \frac{z_{\beta_\mu} - z_{\alpha_\mu}}{(z - z_{\beta_\mu})(z - z_{\alpha_\mu})} ; \quad \mu = 0, 1, \dots, m , \quad (4.27)$$

we see that, apart from ω_0 , only those ω_j , $j = 1, \dots, m$, for which either

$$|z_{\beta_j}| \ll |z_i| \ll |z_{\alpha_j}| \quad \text{or} \quad |z_{\alpha_j}| \ll |z_i| \ll |z_{\beta_j}| \quad (4.28)$$

will satisfy the normalization condition (2.11). The other one-forms will integrate to zero, since the contour a encircles either both or none of the singularities of ω_j . In either of the cases (4.28) we find

$$|\omega_\mu(z_i)| \simeq |z_i|^{-1} , \quad (4.29)$$

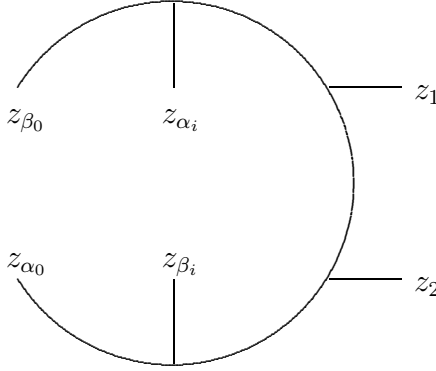


Figure 3: This is a typical representative of the class of Φ^3 diagrams relevant for the Green function $G_{00}^{(m)}$. It corresponds to a particular ordering of the legs z_1 , z_2 , z_{α_i} and z_{β_i} . The other legs (labelled by z_{α_j} and z_{β_j} , $j \neq i$) have been suppressed.

which explicitly shows how all choices of holomorphic one-forms subject to the normalization condition (2.11) are equivalent in the limit $\alpha' \rightarrow 0$. In short, our prescription for the local coordinate reduces in this case to

$$|V_i'(0)| = |z_i| , \quad i = 1, 2 . \quad (4.30)$$

Using the scaling relations (4.24) and (4.26) in eq. (4.17), together with the choice (4.30), we readily recover the particle Green function

$$G_{\text{str}}^{(m)}(z_1, z_2) \xrightarrow{\alpha' \rightarrow 0} \frac{1}{\alpha'} G_{00}^{(m)}(\tau_1, \tau_2) = \frac{1}{\alpha'} \tilde{G}_B^{(m)}(\tau_1, \tau_2) . \quad (4.31)$$

4.2 The Green Function $G_{ii}^{(m)}$

In this case the tree diagram obtained by cutting open all loops consists of the main branch plus the side-branch where the two external legs are inserted (Fig.4). If we choose to let the SPT flow $\tau^{(i)}$ end at the leg labelled by z_{α_i} , we have, according to eq. (2.27)

$$\tau_j^{(i)} = -\frac{\alpha'}{2} \ln \left| \frac{z_j - z_{\alpha_i}}{z_{\alpha_i}} \right| \quad \text{for } j = 1, 2 . \quad (4.32)$$

Here $\tau^{(i)} = 0$ corresponds to the point $\tau = \tau_{\alpha_i}$ on the fundamental loop, whereas $\tau^{(i)} = \bar{T}_i$

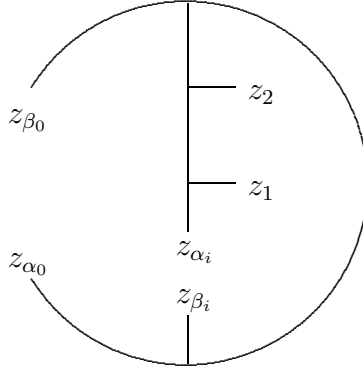


Figure 4: The typical Φ^3 diagram relevant for the Green function $G_{ii}^{(m)}$. The legs labelled by z_{α_j} and z_{β_j} , $j \neq i$, have been suppressed.

corresponds to the point $\tau = \tau_{\beta_i}$, in accordance with the conventions ⁷ underlying the particle Green functions of section 3. We then have the pinching limit

$$\begin{aligned} |z_1 - z_{\alpha_i}| &\ll |z_2 - z_{\alpha_i}| \ll |z_{\alpha_i}| \quad \text{if} \quad \tau_1^{(i)} > \tau_2^{(i)} \\ |z_2 - z_{\alpha_i}| &\ll |z_1 - z_{\alpha_i}| \ll |z_{\alpha_i}| \quad \text{if} \quad \tau_2^{(i)} > \tau_1^{(i)} . \end{aligned} \quad (4.33)$$

In this case the homology cycle a is simply equal to the basis cycle a_i in the homology basis dual to the basis (4.27) of holomorphic one-forms, and accordingly we may take

$$|V'_j(0)| = |\omega_i(z_j)|^{-1} = \left| \frac{(z_j - z_{\alpha_i})(z_j - z_{\beta_i})}{z_{\alpha_i} - z_{\beta_i}} \right| \simeq |z_j - z_{\alpha_i}| \quad \text{for } j = 1, 2 . \quad (4.34)$$

It is now straightforward to verify that in the pinching limit (4.33)

$$\begin{aligned} \ln \left| \frac{z_1^{1/2} z_2^{1/2}}{(V'_1(0))^{1/2} (V'_2(0))^{1/2}} \right| + G_{\text{str}}^{(0)}(z_1, z_2) &\simeq \\ \ln \left| \frac{(z_1 - z_{\alpha_i}) - (z_2 - z_{\alpha_i})}{(z_1 - z_{\alpha_i})^{1/2} (z_2 - z_{\alpha_i})^{1/2}} \right| &\xrightarrow{\alpha' \rightarrow 0} \frac{1}{\alpha'} |\tau_1^{(i)} - \tau_2^{(i)}| , \end{aligned} \quad (4.35)$$

while for $j = 1, 2$ and $k = 1, \dots, m$

$$G_{\text{str}}^{(0)}(z_j, z_{\beta_k}) \xrightarrow{\alpha' \rightarrow 0} \frac{1}{\alpha'} G_B(\tau_{\alpha_i}, \tau_{\beta_k}) ,$$

⁷It is, of course, possible to adopt the reverse notation, which corresponds to the interchange of $\alpha_i \leftrightarrow \beta_i$. We verified that the relation between string and particle Green functions remains unchanged, as long as a similar change of convention is adopted in the particle formulae eqs. (3.22), (3.23).

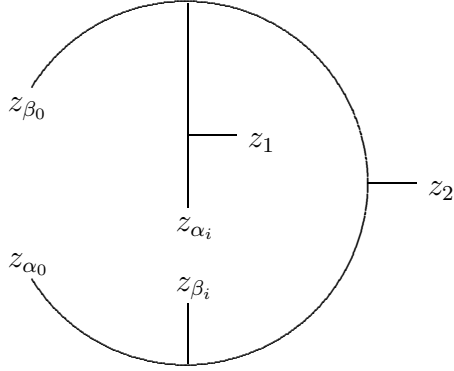


Figure 5: The typical Φ^3 diagram relevant for the Green function $G_{i0}^{(m)}$. The legs labelled by z_{α_j} and z_{β_j} , $j \neq i$, have been suppressed.

$$G_{\text{str}}^{(0)}(z_j, z_{\alpha_k}) \xrightarrow{\alpha' \rightarrow 0} \frac{1}{\alpha'} \left\{ G_B(\tau_{\alpha_i}, \tau_{\alpha_k})(1 - \delta_{ik}) - 2\tau_j^{(i)} \delta_{ik} \right\} ,$$

so that

$$X_{\text{str}}(z_1, z_2; z_{\alpha_k}, z_{\beta_k}) \xrightarrow{\alpha' \rightarrow 0} -\frac{2}{\alpha'}(\tau_1^{(i)} - \tau_2^{(i)})\delta_{ik} . \quad (4.36)$$

Combining eqs.(4.35), (4.36) and (4.24) we find

$$G_{\text{str}}^{(m)}(z_1, z_2) \xrightarrow{\alpha' \rightarrow 0} \frac{1}{\alpha'} G_{ii}^{(m)}(\tau_1^{(i)}, \tau_2^{(i)}) , \quad (4.37)$$

as desired.

4.3 The Green Function $G_{i0}^{(m)}$

This case is a mixture of the previous two (Fig.5). We have

$$\begin{aligned} \tau_1^{(i)} &= -\frac{\alpha'}{2} \ln \left| \frac{z_1 - z_{\alpha_i}}{z_{\alpha_i}} \right| & |V_1'(0)| &= |z_1 - z_{\alpha_i}| \\ \tau_2 &= -\frac{\alpha'}{2} \ln |z_2| & |V_2'(0)| &= |z_2|, \end{aligned} \quad (4.38)$$

and in the relevant pinching limit ($|z_2| \ll 1$ and $|z_1 - z_{\alpha_i}| \ll |z_{\alpha_i}| \ll 1$) we find

$$\ln \left| \frac{z_1^{1/2} z_2^{1/2}}{(V'_1(0))^{1/2} (V'_2(0))^{1/2}} \right| + G_{\text{str}}^{(0)}(z_1, z_2) \xrightarrow{\alpha' \rightarrow 0} \frac{1}{\alpha'} \left[G_B(\tau_{\alpha_i}, \tau_2) + \tau_1^{(i)} \right] \quad (4.39)$$

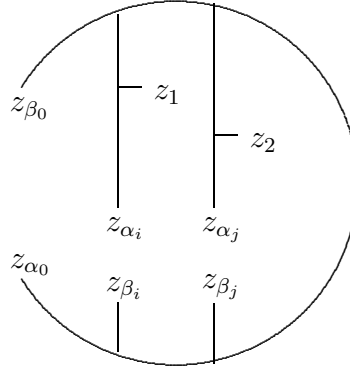


Figure 6: The typical Φ^3 diagram relevant for the Green function $G_{ij}^{(m)}$. The legs labelled by z_{α_k} and z_{β_k} , $k \neq i, j$, have been suppressed.

$$X_{\text{str}}(z_1, z_2; z_{\alpha_j}, z_{\beta_j}) \xrightarrow{\alpha' \rightarrow 0} \frac{2}{\alpha'} \left[X(\tau_{\alpha_i}, \tau_2; \tau_{\alpha_j}, \tau_{\beta_j}) - \tau_1^{(i)} \delta_{ij} \right] , \quad (4.40)$$

which, combined with eq. (4.24), leads to the correct result, i.e. that

$$G_{\text{str}}^{(m)}(z_1, z_2) \xrightarrow{\alpha' \rightarrow 0} \frac{1}{\alpha'} G_{i0}^{(m)}(\tau_1^{(i)}, \tau_2) . \quad (4.41)$$

4.4 The Green Function $G_{ij}^{(m)}$ ($i \neq j$)

In this case, when we cut open the loops of the Φ^3 -diagram, we have two side-branches inserted on the main branch: one ending at z_{α_i} , with a stem labelled by z_1 ; and another ending at z_{α_j} , with a stem labelled by z_2 (Fig.6). The mapping into SPTs and the choice of local coordinates are as follows

$$\begin{aligned} \tau_1^{(i)} &= -\frac{\alpha'}{2} \ln \left| \frac{z_1 - z_{\alpha_i}}{z_{\alpha_i}} \right| & |V_1'(0)| &= |z_1 - z_{\alpha_i}| \\ \tau_2^{(j)} &= -\frac{\alpha'}{2} \ln \left| \frac{z_2 - z_{\alpha_j}}{z_{\alpha_j}} \right| & |V_2'(0)| &= |z_2 - z_{\alpha_j}| , \end{aligned} \quad (4.42)$$

and in the pinching limit $|z_1 - z_{\alpha_i}| \ll |z_{\alpha_i}|$ and $|z_2 - z_{\alpha_j}| \ll |z_{\alpha_j}|$ we find

$$\ln \left| \frac{z_1^{1/2} z_2^{1/2}}{(V_1'(0))^{1/2} (V_2'(0))^{1/2}} \right| + G_{\text{str}}^{(0)}(z_1, z_2) \xrightarrow{\alpha' \rightarrow 0} \frac{1}{\alpha'} \left[G_B(\tau_{\alpha_i}, \tau_{\alpha_j}) + \tau_1^{(i)} + \tau_2^{(j)} \right] \quad (4.43)$$

$$X_{\text{str}}(z_1, z_2; z_{\alpha_k}, z_{\beta_k}) \xrightarrow{\alpha' \rightarrow 0} \frac{2}{\alpha'} \left[X(\tau_{\alpha_i}, \tau_{\alpha_j}; \tau_{\alpha_k}, \tau_{\beta_k}) - \tau_1^{(i)} \delta_{ik} + \tau_2^{(j)} \delta_{jk} \right] , \quad (4.44)$$

and thus, as expected

$$G_{\text{str}}^{(m)}(z_1, z_2) \xrightarrow{\alpha' \rightarrow 0} \frac{1}{\alpha'} G_{ij}^{(m)}(\tau_1^{(i)}, \tau_2^{(j)}) . \quad (4.45)$$

5 Conclusions and Open Problems

We have described how the particle Green function (corresponding to any given Φ^3 vacuum diagram) can be obtained from the string Green function by approaching the corner in string moduli space where the string world sheet degenerates into the desired particle diagram, more precisely, by taking the limit $\alpha' \rightarrow 0$, keeping all Schwinger Proper Times of the particle diagram fixed at finite values.

Since the string Green function is not conformally invariant, one will only recover the particle Green function in this limit if an appropriate choice is made for the set of local coordinates, more precisely, for the quantities $|V'_i(0)|$, in the limit of degenerate string world sheets. We have prescribed how to make this choice.

We have also given a set of simple rules, formulated in the explicit setting of the Schottky parametrization, that allows one to identify the corner of string moduli space corresponding to any given N -point multiloop Φ^3 particle diagram, as well as the precise mapping of string moduli into the Schwinger Proper Times pertaining to such a diagram.

Our general procedure has been verified by explicit comparison with all types of particle world-line Green functions corresponding to the Schmidt-Schubert class of Φ^3 vacuum diagrams.

Although we have chosen to express the world-line Green functions in terms of the SPT parameters T of the fundamental loop and \bar{T}_i of the internal propagators, generally speaking there is no unique way of introducing the SPT parametrization for a given particle diagram. However, the prescription we have given for taking the field theory limit is entirely geometrical and therefore should not depend on the choice of SPT parametrization. Accordingly, although a different choice of SPT parametrization will lead to a new world-line Green function, this new Green function should be related to the old one

merely by the appropriate change of SPT variables, as discussed in the two-loop case in ref. [16].

Understanding how the bosonic world-line Green function of particle theory is recovered from the world-sheet Green function of string theory is obviously a relevant step towards the formulation of string-based rules for multiloop amplitudes in *any* field theory.

In the case of Φ^3 theory, analyzed from the particle point of view in ref. [6] and from the string point of view in ref. [19], it constitutes the major part of such a formulation.

However, in the physically more interesting case of Yang-Mills theory, various obstacles remain. First of all, the structure of the 3-point interactions is much more complicated than in Φ^3 theory. In string theory this new structure of the scattering amplitudes arises in various ways: In the bosonic string [18],[17] it appears as a result of having to expand the modular integrand around the tachyon poles in order to obtain the massless poles. In the superstring [1], it appears as a result of having also fermionic fields on the world-sheet. In either case, some severe problems arise at multiloop level. In the bosonic string, the subtraction of the tachyon poles introduces potential ambiguities in the remaining massless amplitude [20]. In the superstring one has to deal with either an integration over supermoduli [9] or the insertion of picture changing operators [10]. Either way, one will face the problem of total derivatives, making the explicit analysis potentially ambiguous and at any rate very delicate.

Another complication of Yang-Mills theory as compared to Φ^3 theory is the existence of contact terms. At one-loop level all contact terms may be removed by a partial integration with respect to the Koba-Nielsen variables [1], but, as argued in detail in ref. [10], this does not seem to be possible at multiloop level. Contact term contributions to the amplitude can arise from string world sheets that are *not* fully pinched, i.e. where two vertices need not be separated by an (almost) infinitely long cylinder. Therefore, to extract all contact terms from the string theory amplitude one needs to integrate not only over the various “ Φ^3 -like” corners of moduli space that we have investigated in this paper, but also over appropriate parts of moduli space interpolating between these corners. A tractable way of doing this has yet to be found.

A Proof of eqs. (3.19) and (3.20)

In this Appendix we present a proof of the two identities (3.19) and (3.20) quoted in section 3. We start from the defining relation of $G_B^{(m)}$ (given by eq.(16) in ref. [6])

$$G_B^{(m)}(\tau_1, \tau_2) = G_B(\tau_1, \tau_2) + \frac{1}{2} \sum_{k=1}^m \bar{T}_k^{-1} g_k^{(m)}(\tau_1) g_k(\tau_2) , \quad (\text{A.1})$$

where

$$g_k^{(m)}(\tau) \equiv G_B^{(m)}(\tau, \tau_{\alpha_k}) - G_B^{(m)}(\tau, \tau_{\beta_k}) , \quad (\text{A.2})$$

with the understanding that $g_k = g_k^{(0)}$ and $G_B^{(0)} = G_B$. The relation (A.1) is very useful for checking various algebraic identities concerning $G_B^{(m)}$, since it does not involve explicitly the inverse of the matrix A .

In addition, we list the following algebraic relations which can be shown directly from the definitions (3.17), (3.18), (3.2) and (3.4).

$$X_{ij}^{(m)} = X_{ji}^{(m)} = X_{ij} + \sum_{k,l=1}^m X_{ik} A_{kl}^{-1} X_{lj} , \quad (\text{A.3})$$

$$X_{ii}^{(m)} = -\tilde{G}_B^{(m)}(\tau_{\alpha_i}, \tau_{\beta_i}) , \quad (\text{A.4})$$

$$\begin{aligned} X^{(m)}(a, b; c, d) &= -X^{(m)}(b, a; c, d) = -X^{(m)}(a, b; d, c) \\ &= X^{(m)}(b, a; d, c) = X^{(m)}(c, d; a, b) . \end{aligned} \quad (\text{A.5})$$

Now, applying eq. (A.1) to the definition (3.17) we obtain

$$X^{(m)}(\tau_a, \tau_b; \tau_c, \tau_d) = X(\tau_a, \tau_b; \tau_c, \tau_d) + \sum_{k=1}^m \bar{T}_k^{-1} X_k^{(m)}(\tau_a, \tau_b) X_k(\tau_c, \tau_d) . \quad (\text{A.6})$$

Since both $X^{(m)}$ and X are symmetric under the interchange $(\tau_a, \tau_b) \leftrightarrow (\tau_c, \tau_d)$, so is the second term on the right-hand side of eq. (A.6). This allows us to write eq. (A.6) on the alternative form

$$X^{(m)}(\tau_a, \tau_b; \tau_c, \tau_d) = X(\tau_a, \tau_b; \tau_c, \tau_d) + \sum_{k=1}^m \bar{T}_k^{-1} X_k(\tau_a, \tau_b) X_k^{(m)}(\tau_c, \tau_d) . \quad (\text{A.7})$$

We are now in a position to verify the formula for the inverse matrix, A^{-1} , given by eq. (3.19). Multiplying the right-hand side of this equation by A , as defined in eq. (3.3), and using eq. (A.6), we immediately find

$$\sum_{k=1}^m \frac{1}{\bar{T}_i \bar{T}_k} (\bar{T}_i \delta_{ik} + X_{ik}^{(m)}) A_{kj} = \delta_{ij} + \frac{1}{\bar{T}_i} \left(X_{ij}^{(m)} - X_{ij} - \sum_{k=1}^m \frac{1}{\bar{T}_k} X_{ik}^{(m)} X_{kj} \right) = \delta_{ij} .$$

The notations X_{ij} and X_k are explained in eqs. (3.18) and (3.24).

Next, to prove eq. (3.20) we use eq. (A.7), according to which

$$\begin{aligned} X^{(m)}(\tau_a, \tau_b; \tau_{\alpha_i}, \tau_{\beta_i}) &= X(\tau_a, \tau_b; \tau_{\alpha_i}, \tau_{\beta_i}) + \sum_{k=1}^m \frac{1}{\bar{T}_k} X_k^{(m)}(\tau_{\alpha_i}, \tau_{\beta_i}) X_k(\tau_a, \tau_b) \\ &= \sum_{k=1}^m \left(\frac{1}{\bar{T}_k} X_{ik}^{(m)} + \delta_{ik} \right) X_k(\tau_a, \tau_b) \\ &= \bar{T}_i \sum_{k=1}^m A_{ik}^{-1} X_k(\tau_a, \tau_b) , \end{aligned} \quad (\text{A.8})$$

where eq. (3.19) is used at the bottom line. This proves eq. (3.20).

References

- [1] Z. Bern and D.A. Kosower, *Nucl. Phys.* **B379** (1992) 451.
- [2] Z. Bern and D.C. Dunbar, *Nucl. Phys.* **B379** (1992) 562.
- [3] Z. Bern, D.C. Dunbar and T. Shimada, *Phys. Lett.* **B312** (1993) 277;
D.C. Dunbar and P.S. Norridge, *Nucl. Phys.* **B433** (1995) 181.
- [4] M.J. Strassler, *Nucl. Phys.* **B385** (1992) 145.
- [5] D.G.C. McKeon, *Ann. Phys.* **224** (1993) 139;
D.G.C. McKeon and A. Rebhan, *Phys. Rev.* **D48** (1993) 2891;
C.S. Lam, *Phys. Rev.* **D48** (1993) 873;
D. Cangemi, E. D'Hoker and G. Dunne, *Phys. Rev.* **D51** (1995) 2513;
E. D'Hoker and D.G. Gagné, hep-th/9508131;
J.W. van Holten, *Z. Phys.* **C66** (1995) 303; *Nucl. Phys.* **B457** (1995) 375;
M.G. Schmidt and C. Schubert, *Phys. Lett.* **B318** (1993) 438;
M. Mondragón, L. Nellen, M.G. Schmidt and C. Schubert, *Phys. Lett.* **B351** (1995) 200;
Phys. Lett. **B366** (1996) 212.
- [6] M.G. Schmidt and C. Schubert, *Phys. Lett.* **B331** (1994) 69.
- [7] M.G. Schmidt and C. Schubert, *Phys. Rev.* **D53** (1996) 2150.
- [8] K. Daikouji, M. Shino and Y. Sumino, *Phys. Rev.* **D53** (1996) 4598.
- [9] K. Roland, *Phys. Lett.* **B289** (1992) 148.
- [10] K. Roland, SISSA/ISAS 131-93-EP preprint.
- [11] E. Martinec, *Nucl. Phys.* **B281** (1987) 157.
- [12] P. Di Vecchia, M.L. Frau, K. Hornfeck, A. Lerda, F. Pezzella and S. Sciuto, *Nucl. Phys.* **B322** (1989) 317.

- [13] A.M. Polyakov, "Gauge Fields and Strings" (Harwood,1987).
- [14] A. Bellini, G. Cristofano, M. Fabbrichesi and K. Roland, *Nucl. Phys.* **B356** (1991) 69.
- [15] J.L. Petersen and J.R. Sidenius, *Nucl. Phys.* **B301** (1988) 247.
- [16] H-T. Sato, *Phys. Lett.* **B371** (1996) 270.
- [17] P. Di Vecchia, A. Lerda, L. Magnea, R. Marotta and R. Russo, NORDITA 95/85-P DFTT 81/95 preprint, hep-th/9601143.
- [18] Z. Bern, *Phys. Lett.* **B296** (1992) 85.
- [19] P. Di Vecchia, A. Lerda, L. Magnea, R. Marotta and R. Russo, DFTT 41/96 preprint, hep-th/9607141.
- [20] Z. Bern and K. Roland, unpublished. *Phys. Rev. Lett.* **70** (1993) 2677.